

Kinetics and Mechanism of Oxidation of the Drug Intermediate 1-(2-Hydroxyethyl)piperidine by Bis(hydrogenperiodato)argentate(III)

Hongmei Shi,^{*,a} Jiong Zhang,^b Shuying Huo,^b Shigang Shen,^b
Weijun Kang^a and Tiesheng Shi^{*,b}

^aSchool of Public Health, Hebei Medical University, Shijiazhuang 050017, Hebei, China

^bCollege of Chemistry and Environmental Science and the Key Laboratory of Medicinal Chemistry and Molecular Diagnostics (MOE), Hebei University, Baoding 071002, Hebei, China

1-(2-Hidroxietil)piperidina (HEP) está presente em muitos fármacos e em protótipos de fármacos, mas seus mecanismos de oxidação são mal compreendidos. Assim, a reação de oxidação da HEP pelo bis(hidrogenoperiodato)-argentato(III) ($[\text{Ag}(\text{HIO}_6)_2]^{5-}$) foi investigada em meio alcalino aquoso. Piperidina e formaldeído foram identificados como principais produtos da reação através da técnica de espectrometria de massa com ionização *electrospray*. A cinética de oxidação foi acompanhada espectrofotometricamente no intervalo de temperatura de 25,0 a 40,0 °C, verificando-se que a reação é de primeira ordem em $[\text{Ag}(\text{III})]$ e de ordem fracionária em $[\text{HEP}]$. O estudo da dependência das constantes de velocidade k_{obsd} em relação a $[\text{OH}^-]$ e $[\text{IO}_4^-]_{\text{tot}}$ (concentração de periodato total) possibilitou estabelecer uma lei de velocidade e propor um mecanismo de reação. O mecanismo envolve a formação do complexo ternário periodato-Ag(III)-HEP, seguido de sua decomposição a Ag(I) através de dois caminhos: um independente e outro facilitado por OH^- . As constantes de velocidade e de equilíbrio bem como os parâmetros de ativação correspondentes às etapas determinantes de velocidade foram calculados.

1-(2-Hydroxyethyl)piperidine (HEP) is involved in many drugs and drug leads, but its oxidation mechanisms are poorly understood. The oxidation of HEP by bis(hydrogenperiodato)-argentate(III) ($[\text{Ag}(\text{HIO}_6)_2]^{5-}$) in aqueous alkaline medium was shown, by electrospray ionization mass spectrometry (ESI-MS), to generate piperidine and formaldehyde as the major products. The reaction was monitored spectrophotometrically in the 25.0 to 40.0 °C range revealing that the oxidation followed a first-order kinetics in $[\text{Ag}(\text{III})]$ and a fractional-order in $[\text{HEP}]$. A rate law and a reaction mechanism were proposed based on the study of the dependency of the pseudo-first-order rate constants, k_{obsd} , on $[\text{OH}^-]$ and on $[\text{IO}_4^-]_{\text{tot}}$ (total concentration of periodate). The mechanism involves the formation of a periodato-Ag(III)-HEP ternary complex, whose decomposition generates Ag(I) by means of two pathways: one independent and another facilitated by OH^- . The reaction rate constants and associated equilibrium constants as well as the activation parameters of the rate-determining steps were calculated.

Keywords: 1-(2-hydroxyethyl)piperidine, Ag(III), oxidation, kinetics, mechanism

Introduction

It is not exaggerated at all to describe 1-(2-hydroxyethyl)-piperidine (HEP) as an important drug intermediate since it is involved in several clinical drugs and in many newly developed drug leads. For instance, raloxifene,^{1,2} pipazethate^{3,4} and flavoxate,^{5,6} all containing HEP moiety, are currently prescribed drugs. Specifically, raloxifene has been used for treatment and prevention

of osteoporosis in postmenopausal women,^{1,2} whereas pipazethate is a non-narcotic antitussive drug.^{3,4} Flavoxate is an anticholinergic with antimuscarinic effects and has been employed to treat urinary bladder spasms.^{5,6} Also, many drug leads containing HEP moiety, some with functions ranging from anticancer, via anti-estrogen, to anti-inflammatory, can be found in very recent literature.⁷⁻¹⁰

On the other hand, HEP oxidation studies appeared to be very scarce,^{11,12} providing very little mechanistic information. Thus, our group initiated a detailed spectrometric kinetic investigation on the oxidation of HEP

*e-mail: hongmshi@yahoo.com.cn, rock@hbu.edu.cn

by the bis(hydrogenperiodato)argentate(III) complex anion, $[\text{Ag}(\text{HIO}_6)_2]^{5-}$, establishing the rate law and delineating a mechanistic picture.

The structure of $[\text{Ag}(\text{HIO}_6)_2]^{5-}$ and its solution chemistry were well described earlier.¹³⁻¹⁷ In the last few years, our investigations on $[\text{Ag}(\text{HIO}_6)_2]^{5-}$ have led to two important findings: (i) the complex has shown some potential to modify peptides and drugs;^{17,18} (ii) the Ag(III) complex can react with luminol or interact directly with some chemicals of analytical importance producing chemiluminescence. This property has been utilized by us and other researchers to analyze biological samples, such as hormones and some drugs, with unusually high sensitivities.¹⁹⁻²⁴ Meanwhile, we have also paid attention to the kinetic and mechanistic aspects of the Ag(III) oxidation reactions, gaining some insights on the possible oxidation mechanisms.^{17,18,25,26} In this work, we report our spectrometric, kinetic and mechanistic results on the oxidation of HEP by that Ag(III) complex.

Experimental

Instrumentation

Electronic spectra and kinetic measurements were carried out on a UV-Vis spectrophotometer (TU-1901, Beijing Puxi, Inc., Beijing, China) equipped with several cell compartments whose temperature was controlled (± 0.2 °C) by circulating water from a thermostat (BG-chiller E10, Beijing Biotech, Inc., Beijing, China). Mass spectra were recorded on an Agilent 1200/6310 ion trap mass spectrometer equipped with an electrospray ionization (ESI) source.

Chemicals and solutions

HEP and 2,4-dinitrophenylhydrazine (DNPH) were obtained from Sigma-Aldrich (St. Louis, MO, USA). Analytical grade AgNO_3 , KIO_4 , $\text{K}_2\text{S}_2\text{O}_8$, KOH , NaNO_3 , KNO_3 and acrylonitrile were purchased either from Beijing Chemical Reagent Company (Beijing, China) or from Tianjin Chemical Reagent Company (Tianjin, China).

The crystallized $\text{Na}_5[\text{Ag}^{\text{III}}(\text{HIO}_6)_2] \cdot 5\text{H}_2\text{O}$ complex was synthesized using AgNO_3 , KIO_4 , $\text{K}_2\text{S}_2\text{O}_8$, KOH and NaNO_3 according to the procedure reported by Balikungeri *et al.*¹³ Electronic spectrum of aqueous Ag(III) complex solution displayed two absorption maxima at 253 and 362 nm, as previously reported in the literature.¹⁴ The stock solutions were prepared and measurement of the Ag(III) complex concentration was conducted by methods described elsewhere.¹⁸ All solutions were prepared with doubly distilled water.

Kinetic measurements

Kinetic measurements were carried out under pseudo first-order reaction conditions, $[\text{HEP}] \geq 10[\text{Ag}(\text{III})]$, $[\text{IO}_4^-]_{\text{tot}} \geq 10[\text{Ag}(\text{III})]$, where $[\text{IO}_4^-]_{\text{tot}}$ denotes the total concentration of externally added periodate. Reaction was started by mixing equal volumes of the Ag(III) and HEP solutions, previously thermostated for at least 15 min, and the reaction mixture was quickly transferred to a pre-thermostated cell. Appropriate amounts of KOH , KIO_4 and KNO_3 were added to adjust $[\text{OH}^-]$, $[\text{IO}_4^-]_{\text{tot}}$ and ionic strength ($\mu = 0.30$ mol L^{-1} used throughout) of both Ag(III) and HEP solutions.

Figure 1 shows the time-resolved spectra for a set of reaction conditions, and the kinetic curves monitoring the absorbance at 360 nm as a function of time are given in Figure 1 as an insert (data point). The kinetic trace was fitted with single exponential equation (equation 1) using nonlinear least-squares routines, where A_t , A_0 and A_∞ stand for the absorbances at time t , zero and infinity, respectively.

$$A_t = (A_0 - A_\infty) \exp(-k_{\text{obsd}} t) + A_\infty \quad (1)$$

The excellent fitting, shown in Figure 1, demonstrates that the reaction is unequivocally first-order in $[\text{Ag}(\text{III})]$. The observed pseudo-first-order rate constants, k_{obsd} , were calculated from the kinetic traces, and the average values of three independent runs are reported. Standard deviations of k_{obsd} were usually less than 5%.

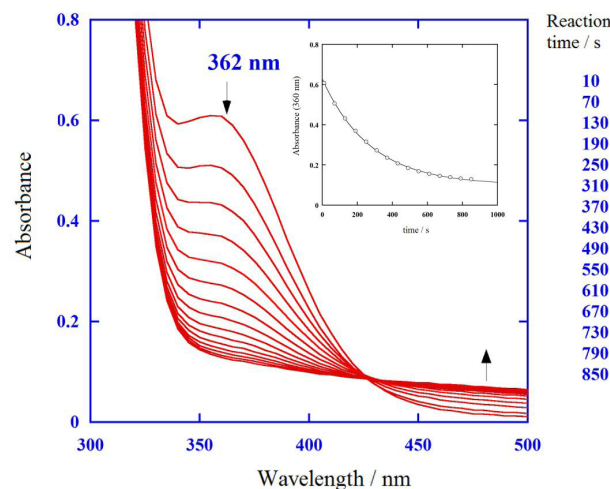


Figure 1. Time-resolved spectra monitoring the reaction between Ag(III) and 1-(2-hydroxyethyl)piperidine (HEP) at 25.0 °C. Conditions: $[\text{Ag}(\text{III})] = 0.05$ mmol L^{-1} , $[\text{HEP}] = 6.0$ mmol L^{-1} , $[\text{OH}^-] = 0.100$ mol L^{-1} , $[\text{IO}_4^-]_{\text{tot}} = 1.00$ mmol L^{-1} and $\mu = 0.30$ mol L^{-1} . The first spectrum was recorded about 10 s after mixing and Δt between scans is 60 s. Inset: a kinetic trace monitoring at 360 nm generated from the time-resolved spectra shown in Figure 1. The solid curved-line represents the best fit of the experimental data using equation 1 and a nonlinear least-square fitting routine.

Test of free radical involvement

A volume of 50 mL of 0.10 mmol L⁻¹ Ag(III) solution containing 0.10 mol L⁻¹ KOH was mixed with 50 mL of 2 mmol L⁻¹ HEP solution containing 8% acrylonitrile in a three neck flask, and stirred for 4 h in N₂ atmosphere. No precipitate of polyacrylonitrile was observed, suggesting that free radicals have not been formed in the reaction. Both solutions were purged for 20 min with nitrogen gas before the reaction.

Identification of the oxidation products

A volume of 100 mL of 1 mmol L⁻¹ Ag(III) solution containing 0.1 mol L⁻¹ KOH was mixed with an equal volume of 10 mmol L⁻¹ HEP solution. After disappearance of the yellow color of the Ag(III) complex indicating the end of the reaction, the reaction mixture was divided in two equal parts. One was extracted with 200 mL of ether, washed once with water and then evaporated to dryness. The residue was dissolved in 2 mL of dilute HCl solution and subjected to mass spectrometry analysis. In the mass spectrum, one of the dominant peaks at *m/z* 86.4 was ascribed to protonated piperidine (piperidine•H⁺), whose calculated *m/z* is 86.15. The minor difference is due to the calibration of the equipment.

An excess of KI and Na₂S₂O₃ was added to the second fraction of the reaction mixture, the pH was adjusted to 5-6 with 1 mol L⁻¹ HCl. In this condition, the periodate was rapidly reduced, giving rise to I₃⁻ which was quickly reduced to iodide by thiosulfite,²⁷ leading to precipitation of AgI and AgCl, after a while. These were filtered off and a saturated solution of DNPH (in 2 mol L⁻¹ HCl) was added to the filtrate. The yellow precipitate, generated after aging the mixture for 2 days in a refrigerator, was washed with water, dissolved in DMSO and analyzed by mass spectrometry. The peak at *m/z* 233 (sodium peak), probably stems from the phenylhydrazone derivative formed by the reaction of DNPH with formaldehyde. Therefore, piperidine and formaldehyde probably are the oxidation products of HEP.

Results and Discussion

Influence of [HEP] on the oxidation rate

The oxidation rate as a function of [HEP] (0.60 ≤ [HEP] ≤ 6.0 mmol L⁻¹) was studied at four temperatures and the plots of *k*_{obsd} vs. [HEP] are displayed in Figure 2. Some simple calculations reveal that the reaction order *n* in [HEP] is fractional, namely 0 < *n* < 1. As a matter of fact, good linear relationships between 1/*k*_{obsd} and 1/[HEP]

were found at all the temperatures (not shown), suggesting that they may follow a Michaelis-Menten type kinetics of enzyme-catalyzed reactions.²⁸ It implies that HEP forms an intermediate complex with Ag(III).

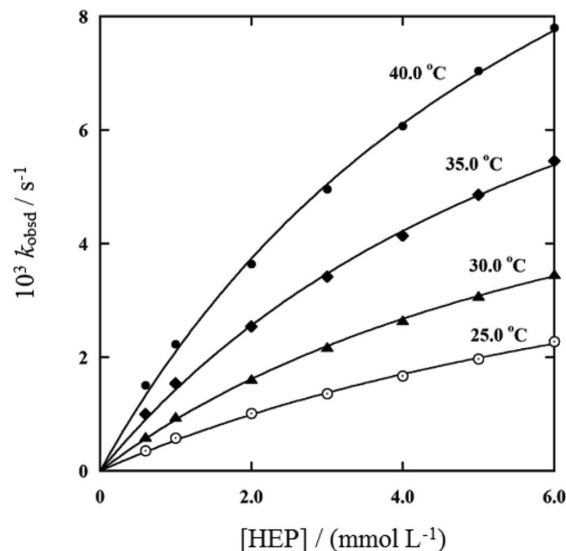


Figure 2. Plots of the observed first-order rate constants, *k*_{obsd}, as a function of [HEP] at different temperatures. Reaction conditions: [Ag(III)] = 0.03 mmol L⁻¹, [IO₄⁻]_{tot} = 1.00 mmol L⁻¹, [OH⁻] = 0.080 mol L⁻¹ and μ = 0.30 mol L⁻¹. The solid lines are the best fits of experimental data by equation 7 using a nonlinear least-squares routine, with *K*₁ = 6.0 × 10⁻⁴ mol L⁻¹ and *f*([OH⁻]) = 0.958.

The time-resolved spectra in Figure 1 show an absorption peak at 360 nm, which is in contrast with 362 nm peak of the Ag(III) complex in pure water. This blue shift of the band suggests that there is an interaction between Ag(III) and HEP, supporting the formation of a complex between Ag(III) and HEP (*vide infra*).

Influence of [OH⁻] on the oxidation rate

The influence of [OH⁻] on the reaction rate was studied in the 0.020 ≤ [OH⁻] ≤ 0.20 mol L⁻¹ range, and the plots of *k*_{obsd} vs. [OH⁻] at different temperatures are shown in Figure 3. The linear plots afforded well-defined and significantly positive intercepts. Similar relationships between *k*_{obsd} and [OH⁻] were observed for the oxidation reactions of (L)-serine and (L)-threonine¹⁸ and mephenesin¹⁷ with Ag(III). But, analogous reactions with (L)-proline and (DL)-pipecolate^{25,26} showed that *k*_{obsd} is essentially independent of [OH⁻].

Influence of [IO₄⁻]_{tot} on the oxidation rate

The influence of [IO₄⁻]_{tot} on *k*_{obsd} was studied in the 0.30 ≤ [IO₄⁻]_{tot} ≤ 2.0 mmol L⁻¹ range, at constant [OH⁻],

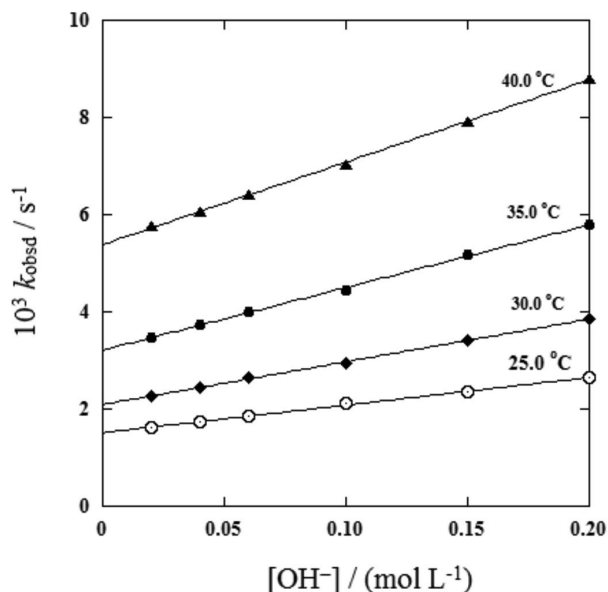
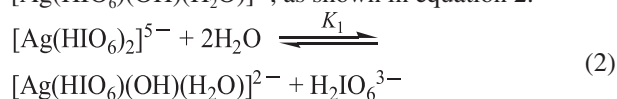


Figure 3. Plots of k_{obsd} against $[\text{OH}^-]$ at four temperatures. Reaction conditions: $[\text{Ag(III)}] = 0.03 \text{ mmol L}^{-1}$, $[\text{IO}_4^-]_{\text{tot}} = 1.00 \text{ mmol L}^{-1}$, $[\text{HEP}] = 5.0 \text{ mmol L}^{-1}$ and $\mu = 0.30 \text{ mol L}^{-1}$.

at 25.0 °C, and the results are listed in Table 1. Obviously, the oxidation rate is significantly decreased when $[\text{IO}_4^-]_{\text{tot}}$ is increased, whereas keeping a linear correlation between $1/k_{\text{obsd}}$ and $[\text{IO}_4^-]_{\text{tot}}$ (figure not shown). Similar behavior was also noticed in the oxidation of different substrates by $[\text{Ag}(\text{HIO}_6)_2]^{5-}$,^{17,18} which was accounted for by a pre-equilibrium (reaction 2) involving $[\text{Ag}(\text{HIO}_6)_2]^{5-}$ and a mono-periodate coordinated silver(III) complex, $[\text{Ag}(\text{HIO}_6)(\text{OH})(\text{H}_2\text{O})]^{2-}$, as shown in equation 2.



In those reactions, $[\text{Ag}(\text{HIO}_6)(\text{OH})(\text{H}_2\text{O})]^{2-}$ was assumed to be the reactive species toward the reductants whereas $[\text{Ag}(\text{HIO}_6)_2]^{5-}$ behaved as a precursor. Presumably, in the present reaction system, $[\text{Ag}(\text{HIO}_6)(\text{OH})(\text{H}_2\text{O})]^{2-}$ is the reactive species also.

Oxidation mechanism

Provided $[\text{Ag}(\text{HIO}_6)(\text{OH})(\text{H}_2\text{O})]^{2-}$ is the reactive species, it should be the intermediate complex formed in the reaction of Ag(III) and HEP, such that the simple expression $k_{\text{obsd}} = a + b[\text{OH}^-]$ can describe the k_{obsd} dependency on $[\text{OH}^-]$ shown in Figure 3. Also, this two-term expression reveals that the oxidation reaction may take place through two channels: one independent of OH^- and another facilitated by that same species. As a consequence, the reaction mechanism shown in Scheme 1 was proposed considering the above observations and hypothesis.

Table 1. Observed and calculated pseudo first-order rate constants, k_{obsd} as a function of $[\text{IO}_4^-]_{\text{tot}}$ at 25.0 °C and 0.30 mol L⁻¹ ionic strength^a

$[\text{IO}_4^-]_{\text{tot}} / (\text{mmol L}^{-1})$	$10^3 k_{\text{obsd}} / \text{s}^{-1} \text{ }^b$	$10^3 k_{\text{obsd}} / \text{s}^{-1} \text{ }^c$
0.20	2.96	2.83
0.30	2.75	2.66
0.40	2.57	2.52
0.50	2.43	2.39
0.70	2.13	2.16
1.00	1.86	1.89
1.30	1.75	1.68
1.50	1.61	1.58
2.00	1.40	1.34

^aMeasured at $[\text{Ag(III)}] = 0.03 \text{ mmol L}^{-1}$, $[\text{HEP}] = 5.0 \text{ mmol L}^{-1}$, $[\text{OH}^-] = 0.080 \text{ mol L}^{-1}$ and $\mu = 0.30 \text{ mol L}^{-1}$. ^bMeasured values. ^cPredicted values.

In this mechanism, the intermediate is proposed to be a ternary complex (structure shown in Scheme 1) formed between $[\text{Ag}(\text{HIO}_6)(\text{OH})(\text{H}_2\text{O})]^{2-}$ and HEP in a pre-equilibrium step. This decomposes to Ag(I) according to two parallel rate-determining steps (described by k_1 and k_2 , respectively).

The rate expression deduced in terms of total concentration of silver(III), $[\text{Ag(III)}]_{\text{tot}}$, where $[\text{H}_2\text{IO}_6^{3-}]_e$ denotes the equilibrium concentration of $\text{H}_2\text{IO}_6^{3-}$, is shown in equation 3.

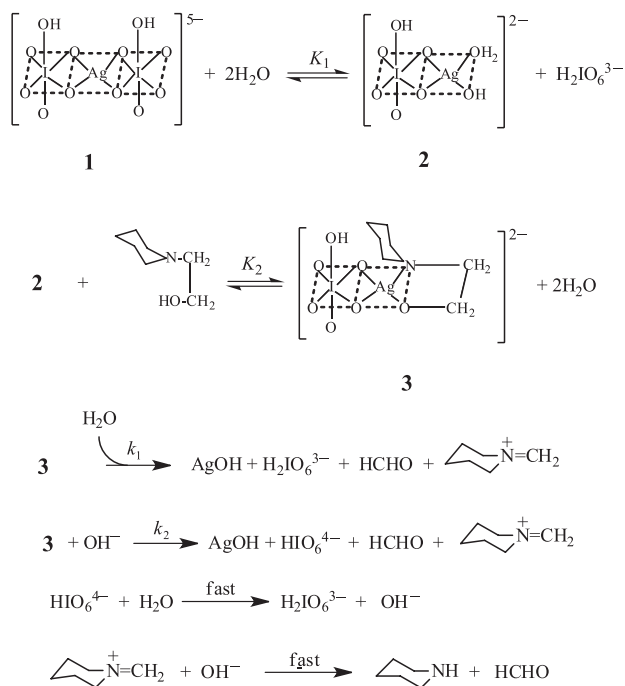
$$-d[\text{Ag(III)}]_{\text{tot}}/dt = k_{\text{obsd}}[\text{Ag(III)}]_{\text{tot}} = \frac{(k_1 + k_2[\text{OH}^-])K_1K_2[\text{HEP}]}{[\text{H}_2\text{IO}_6^{3-}]_e + K_1 + K_1K_2[\text{HEP}]}[\text{Ag(III)}]_{\text{tot}} \quad (3)$$

Hence,

$$k_{\text{obsd}} = \frac{(k_1 + k_2[\text{OH}^-])K_1K_2[\text{HEP}]}{[\text{H}_2\text{IO}_6^{3-}]_e + K_1 + K_1K_2[\text{HEP}]} \quad (4)$$

The kinetic measurements were carried out fulfilling the condition of $[\text{HEP}] \geq 20 [\text{Ag(III)}]_{\text{tot}}$. As a consequence, only a small fraction of HEP is consumed in the formation of ternary complex **3** in Scheme 1. That is estimated to be only 1-3% of the total HEP (less than kinetic standard deviations) such that $[\text{HEP}]$ is essentially the total concentration of HEP in equations 3 and 4.

Periodate speciation in alkaline medium was discussed earlier,^{17,18} suggesting that $\text{H}_2\text{IO}_6^{3-}$ is the predominant species in the studied $[\text{OH}^-]$ range.^{17,18} $[\text{H}_2\text{IO}_6^{3-}]_e$ as a fraction of $[\text{IO}_4^-]_{\text{tot}}$ can be expressed by equations 5 and 6, where β_2 and β_3 are known equilibrium constants of periodate in alkaline medium.^{29,30} The periodate speciation, the equilibrium constants β_2 and β_3 , and more detailed discussions on those parameters are referred to our earlier



Scheme 1. Proposed reaction mechanism.

works.^{17,18} Values of $f([\text{OH}^-])$ as a function of $[\text{OH}^-]$ can be calculated by equation 6.

$$[\text{H}_2\text{IO}_6^{3-}]_e = f([\text{OH}^-])[\text{IO}_4^-]_{\text{tot}} \quad (5)$$

$$f([\text{OH}^-]) = \beta_3[\text{OH}^-]^2 / (1 + \beta_2[\text{OH}^-] + \beta_3[\text{OH}^-]^2) \quad (6)$$

In addition, equation 7 can be derived substituting equation 5 into equation 4:

$$k_{\text{obsd}} = \frac{(k_1 + k_2[\text{OH}^-])K_1K_2[\text{HEP}]}{f([\text{OH}^-])[\text{IO}_4^-]_{\text{tot}} + K_1 + K_1K_2[\text{HEP}]} \quad (7)$$

Rate and equilibrium constants

The pre-equilibrium constant K_1 (equation 7) as a function of temperature was previously derived¹⁸ and is virtually constant in the studied temperature range. Equation 7 was employed to fit the k_{obsd} vs. $[\text{HEP}]$ data

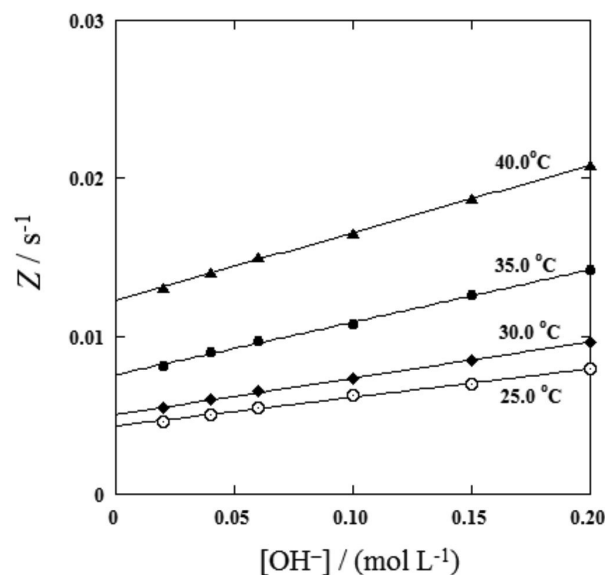
in Figure 2 using a nonlinear least-square method with K_2 and $(k_1 + k_2[\text{OH}^-])$ as adjustable parameters, and $K_1 = 6.0 \times 10^{-4} \text{ mol L}^{-1}$ and $f([\text{OH}^-]) = 0.958$ as constants. The fittings were very good (see Figure 2), and K_2 values derived from the fittings are listed in Table 2.

Equation 7 reformulation gives rise to equation 8:

$$\frac{k_{\text{obsd}} \{f([\text{OH}^-])[\text{IO}_4^-]_{\text{tot}} + K_1 + K_1K_2[\text{HEP}]\}}{K_1K_2[\text{HEP}]} = Z = k_1 + k_2[\text{OH}^-] \quad (8)$$

Thus, values of $Z = k_{\text{obsd}} \{f([\text{OH}^-])[\text{IO}_4^-]_{\text{tot}} + K_1 + K_1K_2[\text{HEP}]\} / K_1K_2[\text{HEP}]$ as a function of $[\text{OH}^-]$ were calculated utilizing the K_2 values. The linear plots of Z against $[\text{OH}^-]$, as anticipated by equation 8 (Figure 4), were used to evaluate the k_1 and k_2 values summarized in Table 2.

Since all rate and equilibrium constants in equation 7 were derived, it is possible to predict or re-calculate the k_{obsd} using the same equation. In this way, k_{obsd} was predicted as a function of $[\text{IO}_4^-]_{\text{tot}}$ and the values given in Table 1. Obviously, the predicted values are in good agreement with the measured ones when the experimental errors are taken

Figure 4. Plots of Z vs. $[\text{OH}^-]$ according to equation 8.Table 2. Derived values of equilibrium constant K_2 , rate constants k_1 and k_2 , and activation parameters

Temperature / °C	k_1 / s^{-1}	$k_2 / (\text{mol}^{-1} \text{L s}^{-1})$	$K_2 / (\text{mol}^{-1} \text{L})$
25.0	$(4.34 \pm 0.06) \times 10^{-3}$	0.0181 ± 0.0005	252 ± 30
30.0	$(5.04 \pm 0.05) \times 10^{-3}$	0.0231 ± 0.0041	334 ± 21
35.0	$(7.57 \pm 0.08) \times 10^{-3}$	0.0333 ± 0.0007	346 ± 36
40.0	0.0123 ± 0.002	0.0427 ± 0.0009	367 ± 38
$\Delta H_1^\ddagger = 52 \pm 9 \text{ kJ mol}^{-1}$		$\Delta H_2^\ddagger = 43 \pm 3 \text{ kJ mol}^{-1}$	
$\Delta S_1^\ddagger = -116 \pm 30 \text{ J K}^{-1} \text{ mol}^{-1}$		$\Delta S_2^\ddagger = -134 \pm 9 \text{ J K}^{-1} \text{ mol}^{-1}$	

into account. Here, it is necessary to stress that the measured k_{obsd} values (Table 1) were not used in the derivation of the rate and equilibrium constants. As a consequence, the good agreement between the measured and predicted k_{obsd} values strongly support the rate law, indicating that the proposed reaction mechanism is reasonable.

Activation parameters

The study of the temperature dependency of k_1 and k_2 enabled the calculation of the corresponding activation parameters. The activation enthalpies and entropies were determined from the Eyring plots shown in Figure 5 (Table 2). The $\Delta H_2^\ddagger = 43 \pm 3 \text{ kJ mol}^{-1}$ and $\Delta S_2^\ddagger = -134 \pm 9 \text{ J K}^{-1} \text{ mol}^{-1}$ are typical for a bimolecular reaction. However, k_1 is still regarded as the first-order rate constant by convention because water concentration is constant, where the bimolecular nature is accounted for by the negative value of ΔS_1^\ddagger . In fact, a one step two-electron transfer process in the rate-determining steps is in line with our free radical involvement test. The reaction intermediate, namely aminium cation in Scheme 1, generated from HEP in the rate-determining steps, is similar to those proposed when ternary amines are oxidized by hypochlorite.³¹

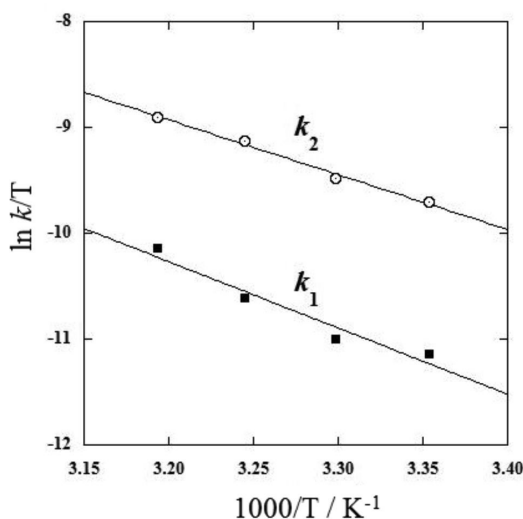


Figure 5. Eyring plots of rate constants k_1 and k_2 .

Conclusions

The reaction products and kinetics for the oxidation of the important drug component HEP by an Ag(III) complex were analyzed by spectrometric techniques. A reaction mechanism involving the indirect formation of a periodato-Ag(III)-HEP ternary complex as an intermediate is supported by both the time-resolved spectra and rate dependence on [HEP]. The ternary complex decomposes

via two reaction channels as the rate-determining steps. The equilibrium constant and rate constants, and their corresponding activation parameters, were evaluated, and a consistent mechanism proposed, enabling the in-depth understanding of the oxidation process. This might be a reference mechanism for the oxidative degradation of the HEP-containing drugs.

Acknowledgement

Financial support of this work by the Natural Science Foundation of China (81273128) is gratefully acknowledged.

References

1. Yu, L.; Liu, H.; Li, W.; Zhang, F.; Luckie, C.; Breemen, R. B. V.; Thatcher, G. R. J.; Bolton, J. L.; *Chem. Res. Toxicol.* **2004**, *17*, 879.
2. Dadiboyena, S.; *Eur. J. Med. Chem.* **2012**, *51*, 17.
3. Abdel-Ghani, N. T.; Shoukry, A. F.; Nashar, R. M. E.; *Analyt* **2001**, *126*, 79.
4. El-Saharty, Y. S.; El-Ragehy, N. A.; Abdel-Monem, H. M.; Abdel-Kawy, M. I.; *J. Adv. Res.* **2010**, *1*, 71.
5. Ruffmann, R.; *J. Int. Med. Res.* **1988**, *16*, 317.
6. El-Gindy, A.; Abdel-Salam, R. A.; Salam, S.; *Drug Dev. Ind. Pharm.* **2008**, *34*, 1311.
7. Casagrande, V.; Salvati, E.; Alvino, A.; Bianco, A.; Ciammaichella, A.; D'Angelo, C.; Ginnari Satriani, L.; Serrilli, A. M.; Iachettini, S.; Leonetti, C.; Neidle, S.; Ortaggi, G.; Porru, M.; Rizzo, A.; Franceschin, M.; Biroccio, A.; *J. Med. Chem.* **2011**, *54*, 1140.
8. Jain, D.; Koh, J. T.; *Bioorg. Med. Chem. Lett.* **2010**, *20*, 5258.
9. Zhou, H. B.; Carlson, K. E.; Stossi, F.; Katzenellenbogen, B. S.; *Bioorg. Med. Chem. Lett.* **2009**, *19*, 108.
10. Khanum, S. A.; Girish, V.; Suqparshwa, S. S.; Khanum, N. F.; *Bioorg. Med. Chem. Lett.* **2009**, *19*, 1887.
11. Smith, J. R. L.; Mead, L. A. V.; *J. Chem. Soc., Perkin 2* **1973**, 1172.
12. Smith, J. R. L.; Masheder, D.; *J. Chem. Soc., Perkin 2* **1977**, 1732.
13. Balikungeri, A.; Pelletier, M.; Monnier, D.; *Inorg. Chim. Acta* **1977**, *22*, 7.
14. Balikungeri, A.; Pelletier, M.; *Inorg. Chim. Acta* **1978**, *29*, 141.
15. Masse, R.; Simon, A.; *J. Solid State Chem.* **1982**, *44*, 201.
16. Levason, W.; *Coord. Chem. Rev.* **1997**, *161*, 33.
17. Shen, S.; Shi, H.; Sun, H.; *Int. J. Chem. Kinet.* **2007**, *39*, 440.
18. Shi, H.; Shen, S.; Sun, H.; Liu, Z.; Li, L.; *J. Inorg. Biochem.* **2007**, *101*, 165.
19. Shi, H.; Xu, X.; Kang, W.; *Anal. Biochem.* **2009**, *387*, 178.

20. Ma, L.; Fan, M.; Xu, X.; Kang, W.; Shi, H.; *J. Braz. Chem. Soc.* **2011**, *22*, 1463.
21. Xu, X.; Zhang, H.; Shi, H.; Ma, C.; Cong, B.; Kang, W.; *Anal. Biochem.* **2012**, *427*, 10.
22. Sun, H.; Chen, P.; Wang, F.; Wen, H.; *Talanta* **2009**, *79*, 134.
23. Rezaei, B.; Ensafi, A. A.; Zarei, L.; *Spectrochimica Acta, Part A* **2012**, *90*, 223.
24. Rezaei, B.; Ensafi, A. A.; Haghghatnia, F.; Aalaye, S. E.; *J. Braz. Chem. Soc.* **2012**, *23*, 2248.
25. Sun, H.; Shi, H.; Shen, S.; Kang, W.; Guo, Z.; *Chin. J. Chem.* **2008**, *26*, 615.
26. Shi, H.; Liu, S.; Shen, S.; Huo, S.; Kang, W.; *Transition Met. Chem.* **2009**, *34*, 821.
27. Afkhami, A.; Madrakian, T.; Zarei, A. R.; *Anal. Sci.* **2001**, *17*, 1199.
28. Wang, W.; Noël, S.; Desmadril, M.; Guéguen, J.; Michon, T.; *Biochem. J.* **1999**, *340*, 329.
29. Aveston, A.; *J. Chem. Soc. A* **1969**, 273.
30. Shi, T. S.; He, J. T.; Ding, T. H.; Wang, A. Z.; *Int. J. Chem. Kinet.* **1991**, *23*, 815.
31. Dennis Jr., W. H.; Hull, L. A.; Rosenblatt, D. H.; *J. Org. Chem.* **1967**, *32*, 3783.

Submitted: March 12, 2013

Published online: July 5, 2013